Effective Capacity of Delay-Constrained Cognitive Radio Links Exploiting Primary Feedback

Ahmed H. Anwar, *Student Member, IEEE*, Karim G. Seddik, *Senior Member, IEEE*, Tamer ElBatt, *Senior Member, IEEE*, and Ahmed H. Zahran, *Member, IEEE*

***Abstract*—In this paper, we study the effective capacity (EC) of cognitive radio (CR) networks operating under statistical quality-of-service (QoS) constraints in an attempt to support real-time applications at the secondary users (SUs). In particular, we analyze the performance gains, in terms of EC and average transmitted power, attributed to leveraging the primary user (PU) feedback overheard at the SU, at no additional complexity or hardware cost. We characterize the EC performance improvement for the SU, in the presence of a feedback-based sensing scheme, under the signal-to-interference-plus-noise ratio (SINR) interference and collision models. Toward this objective, we develop a Markov chain model for feedback-based sensing to compare the performance of a two-link network, a single secondary link, and a primary network abstracted to a single primary link, with and without primary-feedback exploitation. We prove that exploiting the primary feedback at the secondary transmitter improves the EC of the SU under the SINR interference model. On the other hand, interestingly, exploiting the PU feedback messages does not enhance the EC of the SU under the collision model. Nevertheless, exploiting the PU feedback reduces the SU average transmitted power under the two aforementioned models. Finally, we present numerical results, for plausible scenarios, that support our analytical findings.**

***Index Terms*—ARQ Feedback, cognitive radio, collision channel, effective capacity, interference channel, packet delay.**

I. Introduction

WIRELESS communication has become a major challenge worldwide due to the widespread use of handheld and mobile devices and the unprecedented growth of mobile users competing for the limited wireless spectrum. Furthermore, it has been reported by the U.S. Federal Communications Commission that 70% of the "licensed" spectrum goes unutilized in some geographical locations at some time [2]. Cognitive radios (CRs) have been extensively studied over the past decade due to their opportunistic, agile, and efficient spectrum utilization advantages, which enable secondary users (SUs) to use the frequency bands allocated (licensed) to the primary users (PUs), without causing destructive interference. An overview of the CR principals and challenges can be found in [3]–[5].

In a typical CR setting, the secondary transmitter senses the PU activity and then decides whether to access the channel or not, according to the sensing outcome. This setting is problematic in the sense that cognitive users are not aware of their impact on the primary network, apart from the usual sensing errors. Based on [6]–[8], the SU transmitter may exploit information on the PU activity, by overhearing the feedback sent from the primary receiver to the primary transmitter, before sensing the medium. For instance, optimizing the SU channel access decision has been proposed in [9], where Arafa *et al.* investigated the PUs' stability and the SUs' performance by exploiting the PU feedback under the collision model [10]. The idea of exploiting the primary-link automatic repeat request (ARQ) messages is not new, and a similar idea has been studied in [11], where the SUs communicate only during primary ARQ rounds. However, the question is how to utilize the feedback messages. In particular, our system differs in the scheme exploiting the feedback messages. In addition, our prime focus is to characterize the SU performance under statistical delay constraints with the aid of the "effective capacity" (EC) mathematical framework, which was originally introduced in [12]. Other works have considered alternative approaches to improve the SU performance through relaying, for instance, [13].

Supporting quality of service (QoS) has been another daunting challenge for wireless networks. QoS provisions for CR networks, in particular, have received limited attention from the community. Real-time applications targeted by CRs in this paper require QoS provisions, e.g., delay constraints. One approach to mathematically formulate and quantify the impact of delay constraints on the wireless link throughput is the concept of EC [12]. The EC is considered the wireless dual concept to the effective bandwidth, which was originally coined for wired networks in [14].

The EC for interference- and delay-constrained CR relay channels is characterized in [15] under Nakagami fading

Manuscript received December 24, 2014; revised October 4, 2015 and October 11, 2015; accepted October 12, 2015. Date of publication October 26, 2015; date of current version September 15, 2016. This paper was presented in part at the 11th International Symposium on Modeling and Optimization in Mobile, Ad Hoc, and Wireless Networks, Tsukuba Science City, Japan, May 13–17, 2013. This work was supported by the Qatar National Research Fund (a member of Qatar Foundation) under Grant NPRP 4-1034-2-385 and Grant NPRP 09-1168-2-455. The review of this paper was coordinated by Dr. J.-C. Chen.

A. H. Anwar is with the Department of Electrical and Computer Engineering, University of Central Florida, Orlando, FL 32816 USA (e-mail: a.h.anwar@knights.ucf.edu).

K. G. Seddik is with the Department of Electronics and Communications Engineering, American University in Cairo, 11835 New Cairo, Egypt (e-mail: kseddik@aucegypt.edu).

T. ElBatt and A. H. Zahran are with the Department of Electronics and Electrical Communication Engineering, Cairo University, 12613 Giza, Egypt, and also with the Wireless Intelligent Networks Center (WINC), Nile University, 12677 Giza, Egypt (e-mail: telbatt@ieee.org; ahzahran@ieee.org).

Color versions of one or more of the figures in this paper are available online at http://ieeexplore.ieee.org.

Digital Object Identifier 10.1109/TVT.2015.2493040

channels. In [16] and [17], queuing models are employed to evaluate the average delay of packets in CR networks (CRNs), using timeout analysis characteristics. In addition, Musavian and Aissa [18] investigated the CRN fundamental capacity limits with imperfect channel knowledge. In [19], which serves as the baseline for our work, Akin and Gursoy characterized the EC of a CRN under statistical QoS constraints and different assumptions on the availability of channel state information (CSI). Furthermore, exploiting the PU feedback is not incorporated into the model or studied in [19]. In [20], the EC limits for CRNs are established, under peak interference constraints. Moreover, it is shown that for a stricter delay requirement, the EC will not benefit much from relaxing the peak interference constraint. In addition, Shakkottai [21] studied a multiuser formulation of the EC with QoS constraints and proposed a channel-aware greedy scheduling policy as well as a channel-aware max-queue scheduling policy. It has been shown that those algorithms, despite yielding the same long-term throughput in the absence of QoS constraints, exhibit drastically different performance under QoS constraints. However, none of the aforementioned studies have explored the effect of exploiting the PU feedback on the secondary-link EC.

The objective of this work is to address the fundamental question of whether exploiting the PU feedback at the SU enhances its EC and, if so, to what extent. The "feedback part" of the question is triggered by recent evidence in the literature of its strong potential, which has yet to be fully reaped. This is of particular importance since our proposed scheme does not incur any additional complexity or hardware cost. Toward this objective, we utilize the EC as a sound mathematical framework for characterizing the throughput of delay-constrained wireless links.

Our contribution in this work is multifold. First, we model and analyze the impact of overhearing the primary ARQ feedback on the EC of a CR link targeting opportunistic real-time communications. To the best of the authors' knowledge, this is the first attempt toward addressing this problem in the open literature. Second, we conduct a mathematical analysis for the proposed access scheme, based on the theory of nonnegative matrices, under the SINR (interference) and collision models [10]. Third, we establish proofs showing that overhearing the primary-receiver feedback not only enhances the SU EC under the SINR interference model but also reduces its average transmitted power under both models. Finally, we show, with the aid of numerical results, the effect of the PU feedback on the SU EC and average transmitted power while varying the system parameters.

The rest of this paper is organized as follows. A background on the EC is given in Section II. The system model and underlying assumptions are presented in Section III. In Sections IV and V, our main contributions and proofs are introduced, where the EC, with and without primary-feedback exploitation, is analyzed under two interference models. The analysis is conducted under the interference model first since the collision model is considered a special case, as shown later. Afterward, we present the PU performance analysis in Section VI. Finally, the conclusions are drawn and potential directions for future research are pointed out in Section VII.

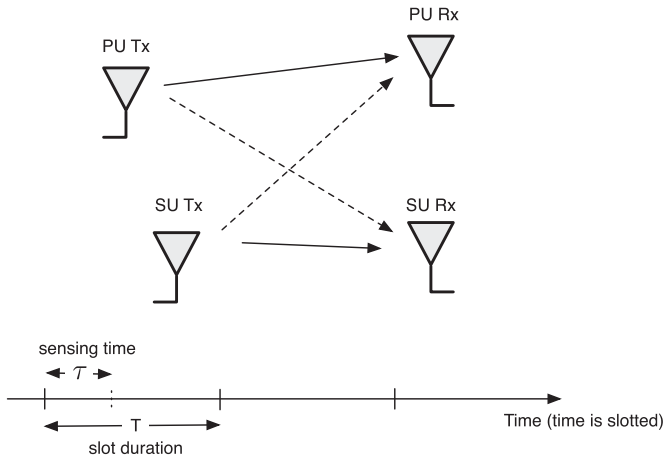

Fig. 1. System model.

II. Background: Effective Capacity

The well-known notion of the information-theoretic capacity, or *channel capacity*, which was established by Shannon in 1948, is defined as the tightest upper bound on the amount of information that can be reliably transmitted over a communication channel [22]. In [12], Wu *et al.* introduced the fundamentally different notion of *EC* of a wireless link as the maximum constant arrival rate that can be supported by a given channel service process while satisfying a statistical QoS requirement specified by the QoS exponent, which is denoted by θ. Hence, the EC concept facilitates capturing the delay constraint of a wireless link without going into complex queuing analysis.

As defined in [12], let Q denote the stationary queue length and θ denote the decay rate of the tail distribution of queue length Q, that is

$$\lim_{q\to\infty} \frac{\log \Pr(Q \geq q)}{q} = -\theta. \tag{1}$$

While θ depends on the arrival and service process statistics, it bounds the maximum delay (or buffer length) that can be supported by a given wireless link and target values of the buffer length violation probabilities. It has been established in [12] that the EC for a given QoS exponent, i.e., θ, is given by

$$-\lim_{t\to\infty} \frac{1}{\theta t} \log_e \mathbb{E}\left\{e^{-\theta \bar{r}(t)}\right\} = -\frac{\Lambda(-\theta)}{\theta} \tag{2}$$

where $\Lambda(\theta) = \lim_{t\to\infty}(1/t)\log_e \mathbb{E}\{e^{\theta \bar{r}(t)}\}$, $\bar{r}(t) = \sum_{k=1}^{t} r(k)$, represents the time accumulated service process, and $\{r(k), k = 1, 2, \ldots\}$ is the stochastic service process.

III. System Model

In this paper, we consider a time-slotted system, as shown in Fig. 1. The primary network is abstracted by a single primary link. We assume a single frequency channel where the primary transmitter accesses the channel whenever it has a packet to send. It is worth noting that our analysis is general enough and holds for an arbitrary number of PUs trying to access the

channel. A single SU attempts to access the medium with a certain policy, to be described later, based on the spectrum sensing outcome. The SU is assumed to have a packet to send at the beginning of each time slot. Data are transmitted in frames of duration T seconds, where each frame fits exactly in a single time slot. We assume that the first τ seconds of the slot duration T are used by the SU to sense the licensed spectrum. Although we consider a system with one frequency channel, as previously noted, the analysis presented in this paper holds for practical settings with multiple orthogonal frequency channels.

Throughout this paper, we refer to the system that exploits the PU feedback messages as the "feedback-aided system." The baseline that does not exploit the PU feedback is simply the "no-feedback system." The EC of both systems is analyzed under the interference and collision models [10]. The SU attempts to transmit packets with power P_1 or P_2 when the channel is sensed as busy or idle, respectively, where $P_1 < P_2$. These power levels correspond to the SU transmission rates, i.e., r_1 and r_2, for busy and idle channels, respectively. Ideally, the medium should be sensed busy when the PU is transmitting, and idle otherwise. However, typical sensing errors incorporated into our model give rise to false-alarm and misdetection events. Simple energy detection [5] is adopted as the spectrum sensing mechanism.

The discrete-time secondary-link input–output equations for idle and busy channels in the ith symbol duration are given, respectively, by

$$y(i) = h(i)x(i) + n(i) \quad i = 1, 2, \ldots \tag{3}$$

$$y(i) = h(i)x(i) + I_p(i) + n(i) \quad i = 1, 2, \ldots \tag{4}$$

where $x(i)$ and $y(i)$ represent the complex-valued secondary-channel input and output, respectively. $h(i)$ denotes the secondary transmitter–receiver channel fading coefficient, $I_p(i)$ is the interference signal from the primary network to the SU, and $n(i)$ is the additive noise at the secondary receiver modeled as a zero-mean circularly symmetric complex Gaussian random variable with variance $\mathbb{E}\{|n(i)|^2\} = \sigma_n^2$. The PU interference on the SU, i.e., $I_p(i)$, is approximated as Gaussian noise with variance $\sigma_{I_p}^2$. The channel bandwidth is denoted W. The channel input is subject to the following average energy constraints: $\mathbb{E}\{|x(i)|^2\} \leq P_1/W$ or $\mathbb{E}\{|x(i)|^2\} \leq P_2/W$, $\forall\, i$, when the channel is sensed busy or idle, respectively. We consider a block-fading channel model and assume that the fading coefficients remain constant for duration T seconds (i.e., one slot duration) and change independently from one slot to another. The fading coefficients are assumed to have an arbitrary distribution with finite variance, that is, $\mathbb{E}\{|h(i)|^2\} = \mathbb{E}\{\zeta(i)\} = \sigma_h^2 < \infty$, where $|h(i)|^2 = \zeta(i)$. We assume that the CSI is available only at the receiver, but not at the transmitter.

A. Feedback-Aided Channel Access Scheme

In the proposed model, we leverage an error-free primary-feedback channel. The primary receiver sends a feedback at the end of each time slot to acknowledge the reception of packets. More specifically, the PU receiver sends an ACK if a packet is correctly decoded or a NACK if the packet is lost. The failure of reception is attributed to the primary-link outage. In case of an idle slot, no feedback is sent. The SU is assumed to overhear this zero-delay primary feedback perfectly (i.e., without errors). Although this assumption is somewhat optimistic, it is justified by the fact that feedback messages are typically short (essentially one bit in our system) and are transmitted over a dedicated control channel that is highly protected by strong channel codes, due to their utmost importance. In addition, this assumption renders the model mathematically tractable and allows us to focus on the fundamental issues at this fresh look at the problem. Nevertheless, the analysis of imperfect feedback is an important extension and is left as a potential subject for future research.

Based on the "overheard" PU feedback, the SU acts as follows: If an ACK/no feedback is heard, the SU normally behaves and starts sensing the channel in the next time slot. However, if a NACK is overheard, the SU transmits with lower power in the next time slot. Thus, "sure" high interference events are avoided in the next slot, since the reception of a NACK triggers the PU to retransmit in the next time slot with probability 1.

We assume that the PU occupies the wireless channel with a fixed prior probability μ [15], [19]. It is well known that the SU spectrum sensing task can be formulated as a binary hypothesis testing problem between the additive white Gaussian noise $n(i)$ and the primary signal $I_p(i)$ added to the noise [23]. Given τW complex symbols in the sensing duration (τ seconds), this can be expressed as

$$H_0 : y(i) = n(i), \quad i = 1, \ldots, \tau W \tag{5}$$

$$H_1 : y(i) = I_p(i) + n(i), \quad i = 1, \ldots, \tau W. \tag{6}$$

We can write down the probabilities of false alarm P_f and detection P_d, which are standard for our system model, as follows:

$$P_f = \Pr(S > \lambda | H_0) = 1 - P\left(\frac{\tau W \lambda}{\sigma_n^2}, \tau W\right) \tag{7}$$

$$P_d = \Pr(S > \lambda | H_1) = 1 - P\left(\frac{\tau W \lambda}{\sigma_{I_p}^2 + \sigma_n^2}, \tau W\right) \tag{8}$$

where λ is the energy detection threshold, $S = (1/\tau W) \sum_{i=1}^{\tau W} |y(i)|^2$ is the test statistic, and $P(x, a)$ denotes the regularized lower gamma function defined as $P(x, a) = (\gamma(x, a))/(\Gamma(a))$, where $\gamma(x, a)$ is the lower incomplete gamma function. The test statistic S is a chi-square distributed random variable with $2\tau W$ degrees of freedom [23].

It is worth noting that our prime focus in this paper is on the SU performance, since exploiting the PU feedback at the SU will not harm the PU. On the contrary, it will always result in an enhanced PU performance, as demonstrated in Section VI, since the extra feedback information will result in "refining" the PU sensing activity at the SU.

In the following two sections, we analyze the SU EC under two interference models.

IV. Effective Capacity Analysis Under the Signal-To-Interference-Plus Noise Ratio Interference Model

Here, we characterize the EC of the SU for the no-feedback and feedback-aided systems, under the SINR Interference model. For the system with no feedback, we present the adopted Markov chain model and then characterize the EC of the SU. The model and analysis are then extended to the feedback-aided system.

The CR setting considered under the SINR interference model can be thought of as a "hybrid" scheme [24], i.e., it is neither a pure underlay nor an interweave CR system. It inherits the channel sensing process from the interweave model. It also coexists with the PU, albeit at lower power levels and rates, following the underlay model. Recall that the medium is busy with a constant PU activity probability, i.e., μ. Next, we develop the Markov chain governing the channel sensing dynamics.

Based on the system model in Section III, the sensing process yields one of four possible outcomes.

1) Channel is busy and detected busy, denoted (B-B): The SU transmits using $\{r_1, P_1\}$, where r_1 and P_1 are the low transmission rate and power, respectively.
2) Channel is busy and detected idle (misdetection), denoted (MD): The SU transmits using the high transmission rate and power, namely, $\{r_2, P_2\}$.
3) Channel is idle and detected busy (false alarm), denoted (FA): The SU transmits using $\{r_1, P_1\}$.
4) Channel is idle and detected idle, denoted (I-I): The SU transmits using $\{r_2, P_2\}$.

By the Gaussian approximation for the PU interference, i.e., $I_p(i)$, we can express the SU instantaneous channel capacity in the given four scenarios as follows:

$$C(i)_l = W \log\left(1 + \text{SNR}_l \zeta(i)\right), \quad l = 1, 2, 3, 4$$

where $\text{SNR}_1 = P_1/(W(\sigma_n^2 + \sigma_{I_p}^2))$, $\text{SNR}_2 = P_2/(W(\sigma_n^2 + \sigma_{I_p}^2))$, $\text{SNR}_3 = P_1/(W(\sigma_n^2))$, and $\text{SNR}_4 = P_2/(W(\sigma_n^2))$.

Assuming that the SU transmitter does not know the CSI, the fixed rates, i.e., r_1 and r_2, may/may not exceed the instantaneous channel capacity, i.e., $C(i)$. Therefore, the channel can be either OFF (outage) or ON, depending on whether the fixed transmission rate exceeds the instantaneous channel capacity or not, respectively, in a given time slot. If the channel is OFF, reliable communication is not attainable, and hence, the packet has to be retransmitted. Thus, an ARQ mechanism is assumed for the SU link to acknowledge the reception of packets and ensure that erroneous data are retransmitted. Accordingly, the effective transmission rate in the OFF states is zero. The Markov chain, which models the different sensing outcomes and channel ON/OFF states, is discussed next.

The Markov chain is fully characterized by its transition probability matrix $\mathbf{R}_{M\times M}$ defined as

$$\mathbf{R}_{M\times M} = [p_{i,j}], \quad 1 \le i, j \le M$$

where M is the number of states. Based on the proof established in [25, Ch. 7] for Markov-modulated processes, the EC for the no-feedback baseline system can be expressed as follows:

$$\text{EC}(\theta) = -\frac{\Lambda(-\theta)}{\theta} = \frac{-1}{\theta}\log_e sp\left(\mathbf{D}(-\theta)\mathbf{R}\right). \tag{9}$$

The matrix $\mathbf{R}$ is the state transition matrix previously defined, where $sp(\mathbf{D}(-\theta)\mathbf{R})$ is the spectral radius of the matrix $\mathbf{D}(-\theta)\mathbf{R}$, that is, the maximum of the absolute of all eigenvalues of the matrix. Thus, to characterize the EC, the problem boils down to deriving the eigenvalues of the matrix $\mathbf{D}(-\theta)\mathbf{R}$. $\mathbf{D}(-\theta)$ is a diagonal matrix defined as $\mathbf{D}(-\theta) = \mathbf{diag}(d_1(-\theta), d_2(-\theta), \ldots, d_M(-\theta))$ whose diagonal elements are the moment-generating functions of the Markov process in each of the M states. Next, we characterize the EC for the system, in case of no-feedback exploitation at the SU.

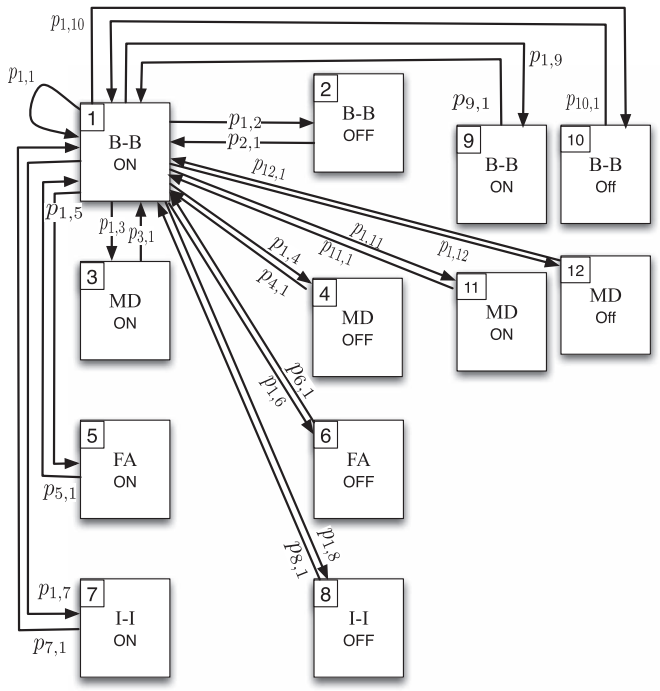

Fig. 2. Markov chain model for the "no-feedback exploitation" system under the SINR interference model.

A. No-Feedback Exploitation (Baseline)

A 12-state Markov chain is constructed to capture all possible sensing outcomes and channel ON/OFF states and incorporate the PU ACK/NACK feedback, as will be illustrated next. This is in contrast to the model developed in [19], which does not consider the PU feedback, our prime interest here. The 12-state Markov chain is shown in Fig. 2, where only the transitions from and into the first state are shown for ease of exposition.

States 1–8 model the system under normal conditions, i.e., when the PU accesses the medium with a fixed prior probability, i.e., μ, as previously mentioned. These eight states simply capture the four possible sensing outcomes (B-B, MD, FA, and I-I) under the two possible channel outage states, namely, ON and OFF. For instance, the system will be in state 1 if the PU is sending a new packet with probability μ; hence, the channel is busy, and the SU successfully detects the PU activity and,

accordingly, sends a secondary packet at low rate and power, i.e., r_1 and P_1. The difference between states 1 and 2 is that at state 1 (ON), $r_1 < C(i)$, whereas at state 2 (OFF), $r_1 > C(i)$. The state transitions are governed by the sensing outcomes, channel instantaneous capacity at each time slot, and the PU feedback, as will be illustrated later.

On the other hand, the last four states (states 9 through 12) capture the subtle differences between the feedback and no-feedback systems. In particular, they model the system when the PU receiver sends a NACK, which changes the behavior of the primary transmitter to retransmit the failed packet with probability 1 (not μ as in normal conditions) in the next time slot.[1] For instance, state 9 (ON) and state 10 (OFF) represent the (B-B) (i.e., correct sensing case), when the PU retransmits. The same argument applies to states 11 (ON) and 12 (OFF), for the (MD) case (i.e., incorrect sensing result) when the PU retransmits. The probability to move into any of the last four states (9–12) will be a function of the primary-link outage probability Pr(outage), which will be characterized in Section VI.

Under the SINR interference model, it should be noted that there exist two different outage probabilities over the primary link, i.e., $\Pr(\text{outage}_1)$ and $\Pr(\text{outage}_2)$, corresponding to the cases where the SU is transmitting with power levels P_1 and P_2, respectively. Based on the assumption that primary-link failure is caused solely by outage, it is straightforward to show that $\Pr(\text{outage}_1) = \Pr(\text{NACK}')$ and $\Pr(\text{outage}_2) = \Pr(\text{NACK}'')$, where $\Pr(\text{NACK}')$ is the probability of overhearing a NACK message from the primary receiver at a given time slot when the SU is transmitting with power P_1 and rate r_1 in that time slot. Similarly, $\Pr(\text{NACK}'')$ is the probability of overhearing a NACK message at any time slot, when the SU is transmitting with power P_2 and rate r_2. Since $P_1 < P_2$, the PU will suffer less interference when the SU is transmitting with the lower power level P_1, and hence, it is evident that $\Pr(\text{NACK}') < \Pr(\text{NACK}'')$. To use the same notation here and in the following section, in which we present the feedback-aided system, we use $\Pr(\text{NACK})$ instead of Pr(outage).

To fully characterize our Markov chain, the transition probabilities are illustrated as follows:

$$\begin{aligned} p_{1,1} &= \mu P_d \Pr(r_1 < C_1(i+TW) | r_1 < C_1(i))(1-\Pr(\text{NACK}')) \\ &= \mu P_d \Pr(\zeta(i+TW) > \nu_1 | \zeta(i) > \nu_1)(1-\Pr(\text{NACK}')) \end{aligned} \tag{10}$$

where $\nu_1 = (2^{r_1/W} - 1)/\text{SNR}_1$, the term $\Pr(r_1 < C_1(i+TW) | r_1 < C_1(i))$ represents the probability that the channel is ON (SU not in outage), μ is the probability of a busy primary channel, P_d is the probability of successful detection as given in (8), and $(1 - \Pr(\text{NACK}'))$ is the probability of no outage in the primary link. Based on the assumption that the channel fading changes independently from one slot to another, $p_{1,1}$ can be further simplified as follows:

$$\begin{aligned} p_{1,1} &= \mu P_d \Pr\left(\zeta(i+TW) > \nu_1\right)\left(1 - \Pr(\text{NACK}')\right) \\ &= \mu P_d \Pr(\zeta > \nu_1)\left(1 - \Pr(\text{NACK}')\right). \end{aligned} \tag{11}$$

Using the relevant events, it can be shown that

$$p_{i,1} = \begin{cases} p_1 = \mu P_d \Pr(\zeta > \nu_1), & i = 5, 6, \ldots, 12 \\ p_1\left(1 - \Pr(\text{NACK}')\right), & i = 1, 2 \\ p_1\left(1 - \Pr(\text{NACK}'')\right), & i = 3, 4 \end{cases} \tag{12}$$

$$p_{i,2} = \begin{cases} p_2 = \mu P_d \Pr(\zeta < \nu_1), & i = 5, 6, \ldots, 12 \\ p_2\left(1 - \Pr(\text{NACK}')\right), & i = 1, 2 \\ p_2\left(1 - \Pr(\text{NACK}'')\right), & i = 3, 4. \end{cases} \tag{13}$$

Similarly

$$p_{i,3} = p_3 = \mu(1 - P_d) \Pr(\zeta > \nu_2), \quad i = 5, 6, \ldots, 12 \tag{14}$$

where $\nu_2 = (2^{r_2/W} - 1)/\text{SNR}_2$, $\nu_3 = (2^{r_1/W} - 1)/\text{SNR}_3$, and $\nu_4 = (2^{r_2/W} - 1)/\text{SNR}_4$.

Similar to states 1 and 2, the transition probabilities for states 4, 5, ..., 8 can be characterized.[2] However, for states 9, 10, 11, and 12, the transition probabilities are different since the probability that the system enters these states is a function of the PU outage probability, i.e.,

$$p_{i,9} = \begin{cases} P_d \Pr(\text{NACK}') \Pr(\zeta > \nu_1), & i = 1, 2 \\ P_d \Pr(\text{NACK}'') \Pr(\zeta > \nu_1), & i = 3, 4 \\ 0, & \text{otherwise} \end{cases} \tag{15}$$

$$p_{i,11} = \begin{cases} (1 - P_d) \Pr(\text{NACK}') \Pr(\zeta > \nu_2), & i = 1, 2 \\ (1 - P_d) \Pr(\text{NACK}'') \Pr(\zeta > \nu_2), & i = 3, 4 \\ 0, & \text{otherwise.} \end{cases} \tag{16}$$

Similar to (15) and (16), we characterize $p_{i,10}$ and $p_{i,12}$ by only changing the probability of the "ON channel" to the "OFF channel."

To simplify the model, we assume that the system never stays in states 9, 10, 11, or 12 for two successive time slots. This assumption implies that the PU has only one retransmission attempt. Despite the fact that this assumption is impractical, we adopt it to avoid packet accumulation in the primary queue. Moreover, this assumption does not affect our main contribution since it is fairly adopted to both systems under investigation. Nevertheless, this assumption can be relaxed to the general case of k transmission attempts, but at the expense of more states, transitions, and, thus, complexity of the adopted Markov chain model. It is also evident that no transitions are permitted from states 5 through 8 to states 9 through 12 since it is impossible for the primary receiver to send a NACK while being idle (i.e., the primary transmitter did not transmit in that slot).

[1] Note that the Markov chain in Fig. 2 is different from the Markov chain in [19] with a different structure for the state transition matrix to incorporate the PU feedback into the model.

[2] The transition probabilities for states 4, 5, ..., 8 are omitted due to space limitations.

It is worth noting that our baseline no-feedback system is not comparable to the system studied in [19]. The main difference is captured in the role of the additional states we have, i.e., states 9, 10, ..., 12. Although both of the systems assume no-feedback overhearing, our proposed system takes into consideration the fact that the behavior of the PU will change in response to the NACK message received from the PU receiver. Specifically, the PU will access the medium with probability 1 when receiving a NACK for retransmission. However, in the system studied in [19], the PU is assumed to access the medium with a fixed probability every time slot from the SU point of view.

By now, we have completely specified the transition probability matrix $\mathbf{R}_{12\times 12}$. The moment-generating function corresponding to each state depends on the effective rate of each state, i.e.,

$$\mathbf{D}(-\theta) = \mathbf{diag}\left\{e^{-(T-\tau)\theta r_1}, 1, e^{-(T-\tau)\theta r_2}, 1, e^{-(T-\tau)\theta r_1}, 1 \; e^{-(T-\tau)\theta r_2}, 1, e^{-(T-\tau)\theta r_1}, 1, e^{-(T-\tau)\theta r_2}, 1\right\}. \quad (17)$$

In the following section, we compare the average power transmitted by the SU under both systems. Thus, the average power transmitted by the SU in case of no-feedback exploitation, which is denoted as P_{avg_N}, can be computed as follows:

$$P_{avg_N} = P_1 \sum_{i=1,2,5,6,9,10} \pi_i + P_2 \sum_{i=3,4,7,8,11,12} \pi_i \quad (18)$$

where π_i is the steady-state probability of state i, and P_1 and P_2 are the SU transmission power values as previously defined.

B. Feedback-Aided Scheme

In case the SU overhears and exploits the PU feedback for channel access, two scenarios arise. First, if the SU overhears a NACK, it does not sense the channel in the next time slot as the PU will retransmit with probability 1. Hence, the SU transmits with low power and rate (i.e., P_1 and r_1) in this slot. On the other hand, if no NACK message is overheard by the SU, it normally behaves (similar to the baseline system) and starts sensing the channel at the beginning of the next time slot, since the PU may or may not be active.

In this system, we construct a ten-state Markov chain, as shown in Fig. 3. States 1 through 8 model exactly the same behavior as the baseline no-feedback exploitation system. On the other hand, states 9 (ON) and 10 (OFF) model the event previously pointed out, which captures the fundamental difference between the two systems, that is, the secondary transmitter overhearing a NACK message from the primary receiver. In essence, overhearing the PU feedback affects the last four states, in Fig. 2, which are reduced to two states corresponding to hearing a primary receiver NACK, as shown in Fig. 3. In the case of overhearing a NACK, misdetections at the SU can never occur (since no sensing is done, and the PU is known to be active); therefore, the last two states (states 11 and 12) in Fig. 2 are not needed in the feedback-aided scheme. Hence, the SU would always transmit with lower power P_1 and rate

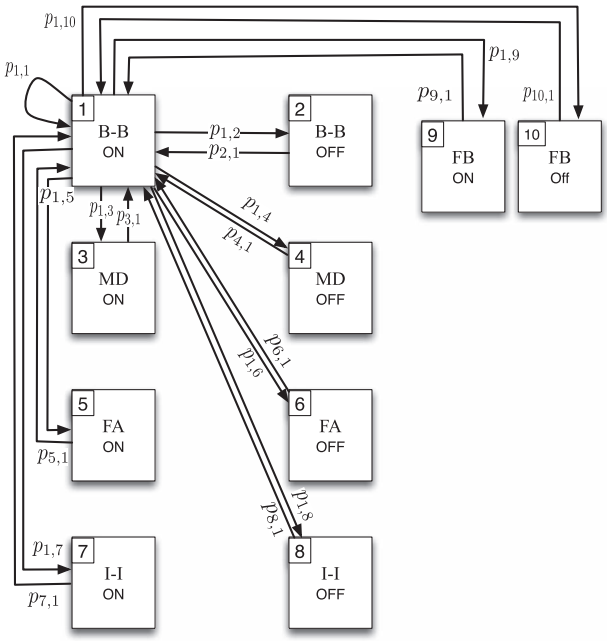

Fig. 3. Markov chain model of the feedback-aided system under the interference model.

r_1 while in states 9 and 10. This, in turn, yields the ten-state Markov chain as follows.

1) States 1–8: B-B, ..., I-I: The behavior in case of ACK/no feedback is exactly similar to the no-feedback exploitation baseline.
2) States 9 and 10: a NACK is heard, (FB): The SU always transmits using $\{r_1, P_1\}$.

Note that the state transition probabilities between the first eight states are the same as the no-feedback exploitation system. This is attributed to the fact that both systems experience exactly the same behavior and dynamics in case of ACK or no feedback. On the other hand, the transition probabilities for states 9 and 10 would be as follows:

$$p_{i,9} = \begin{cases} \Pr(\text{NACK}')\Pr(\zeta > \nu_1), & i = 1,2 \\ \Pr(\text{NACK}'')\Pr(\zeta > \nu_1), & i = 3,4 \\ 0, & \text{otherwise} \end{cases} \quad (19)$$

where $\Pr(\text{NACK}')$ is the probability of hearing a NACK from the primary receiver when the SU transmits is using P_1 and r_1, which is the case at states 1 and 2. $\Pr(\text{NACK}'')$ is the probability of hearing a NACK from the primary receiver when the SU transmits using P_2 and r_2 at states 3 and 4. On the other hand, being at any other state can never cause the SU to overhear a NACK message from the PU and, hence, no transitions from states 5–8 to state 9. Similarly, we characterize $p_{i,10}$ as in (19) by simply changing the probability of the ON channel to the OFF channel.

Accordingly, we construct the transition probability matrix $\mathbf{R}_{10\times 10}$. Since the EC is characterized using the spectral radius of matrix $\mathbf{D}(-\theta)\mathbf{R}$, the moment-generating functions

TABLE I
SYSTEM PARAMETERS

$P_1/W = 0.05$ w/Hz	$P_2/W = 0.1$ w/Hz	$r_1 = 27$ Mbps	$T = 0.1$ msec	$W = 20$ MHz
$r_2 = 54$ Mbps	$r_P = 54$ Mbps	$P_{pu}/W = 1$ w/Hz	$\tau = 0.3 \times T$ sec	$N_0 = 1$
$\mu = 0.7$	$\lambda = 1.85 joules$			

corresponding to each state depend on the effective rate of that state, where

$$\mathbf{D}(-\theta) = \mathbf{diag}\left\{e^{-(T-\tau)\theta r_1}, 1, e^{-(T-\tau)\theta r_2}, 1, e^{-(T-\tau)\theta r_1} \right. \\ \left. 1, e^{-(T-\tau)\theta r_2}, 1, e^{-T\theta r_1}, 1\right\}. \quad (20)$$

The given model and analysis enable us to quantify the CR-link performance gains in terms of EC that is attributed to PU feedback exploitation. The main result of this paper is presented in the following theorem (the proof is given in Appendix A).

Theorem 1: Under the SINR interference model, the EC of the feedback-aided system is always greater than the EC of the no-feedback exploitation system.

C. Average Transmission Power

Along the lines of Section IV-A, the average power transmitted by the SU under the feedback system is given by

$$P_{avg_F} = P_1 \sum_{i=1,2,5,6,9,10} \tilde{\pi_i} + P_2 \sum_{i=3,4,7,8} \tilde{\pi_i} \quad (21)$$

where $\tilde{\pi_i}$ denotes the Markov chain steady-state probability. The numerical results presented in the following section confirm our major findings established in Theorem 1 and provide further insight into the key parameters governing the operation of the proposed feedback-aided access scheme.

D. Numerical Results

Here, we present numerical results that back up our analytical findings and support our main contribution. The values used for the system parameters are given in Table I. Since there is no closed-form expression for the EC, there is no clear guideline on the choice of the rates r_1 and r_2. Hence, we studied the proposed system guided by widely accepted wireless standard parameters for r_1 and r_2, namely, IEEE 802.11g. It should be noted that although the particular choice of rates r_1 and r_2 has an effect on the performance gains due to feedback exploitation, it does not have an effect on the observed trends or relative performance of the studied schemes, backed up by theory (see Theorem 1). The detailed numerical results provide an illustration for the role of our main system parameters, e.g., the delay exponent θ, the sensing duration τ, and the PU activity μ.

Fig. 4 plots the EC for the feedback-aided (FB) and the no-feedback exploitation (No FB) systems versus the delay exponent, i.e., θ. We fix the sensing duration to 30% of the slot duration for which $P_f = 0.304$ and $P_d = 0.84$ according to (7) and (8). Clearly, as delay exponent θ increases (stricter delay requirement), the EC (the maximum rate that the network can sustain in bits per second per hertz) decreases. The same result can be easily distilled from the EC definition in (2). Moreover,

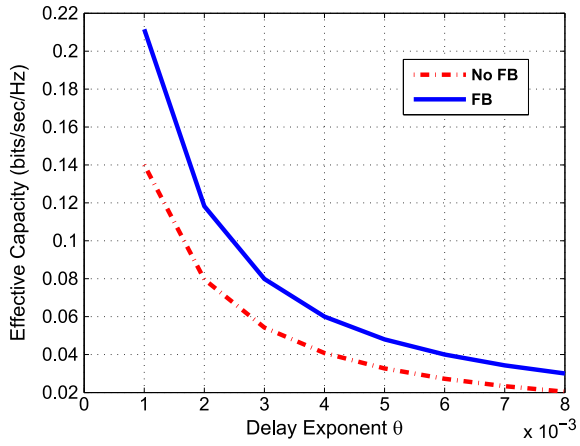

Fig. 4. PU feedback exploitation enhances the EC under the SINR interference model.

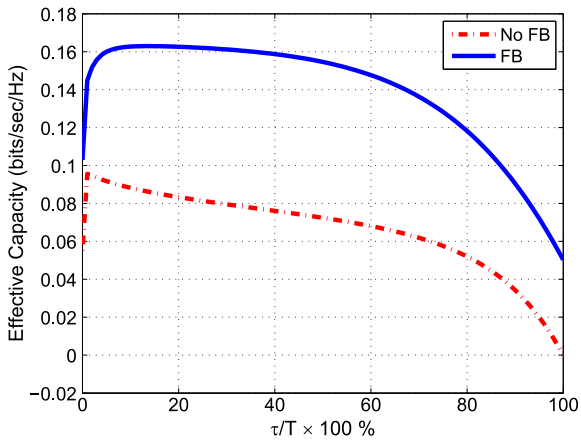

Fig. 5. EC as a function of the sensing-to-slot-duration ratio under the SINR interference model.

it is shown that feedback exploitation yields SU EC gains. As θ increases, the performance gain decreases since the stricter QoS constraint limits the SU throughput, and hence, both systems converge to the maximum arrival rate that can be supported by the secondary link [12].

In Fig. 5, the EC is plotted versus the sensing duration τ, represented as a percentage of the slot duration T. It shows that, for a fixed delay exponent θ and other system parameters, as the sensing duration increases, the portion of the time slot left for data transmission, i.e., $T - \tau$, becomes smaller, yielding lower EC. One may expect that when $\tau = T$, the EC should completely vanish; however, the feedback-aided system still sustains a nonzero EC for the SU. This is attributed to the fact that when the SU overhears a NACK message, it does not sense the medium in the next time slot and sends with power level P_1 and rate r_1, as previously explained, without wasting the time slot in the sensing process.

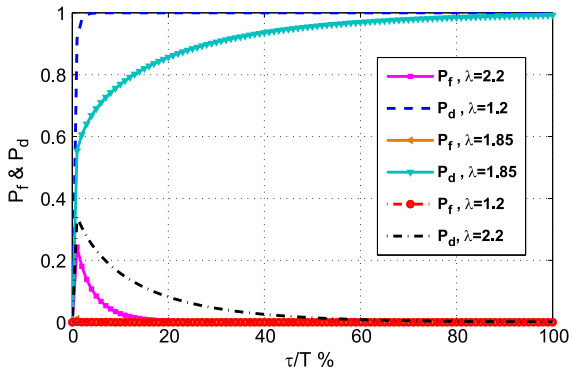

Fig. 6. P_f and P_d as functions of the sensing-to-slot-duration ratio.

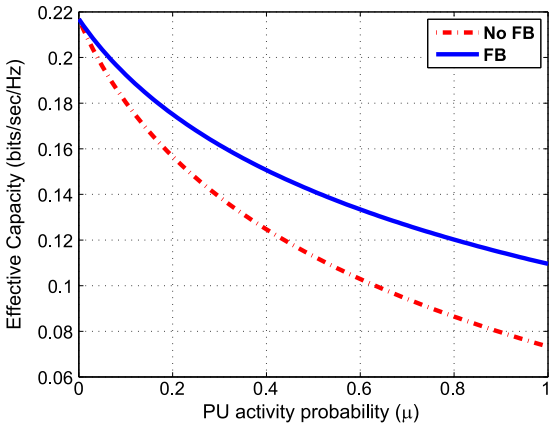

Fig. 7. EC versus PU activity probability μ under the SINR interference model.

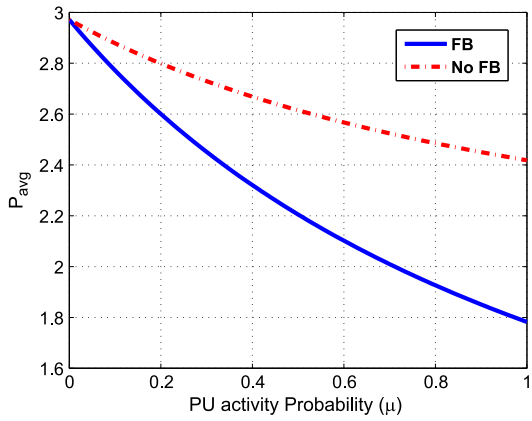

Fig. 8. Average transmission power of the SU versus PU activity probability μ under the SINR interference model.

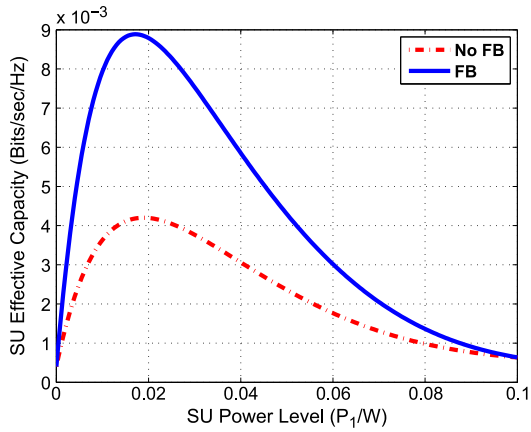

Fig. 9. SU EC versus SU power level P_1 (P_1 from 0 to P_2).

To get a deeper insight into the fundamental tradeoff between sensing accuracy and EC, we plot P_f and P_d versus sensing duration τ, in Fig. 6, for different energy detection thresholds λ.

Obviously, increasing τ enhances the probability of detection and, hence, reduces the sensing errors of false alarm and misdetection. On the other hand, in Fig. 5, we showed that increasing τ reduces the EC as previously explained. This gives rise to a fundamental tradeoff with respect to the optimal sensing duration that strikes a balance between low P_f and P_d (which favors large τ) and saving a large portion of the slot T for data transmission (which favors small τ). Optimizing this tradeoff is out of the scope of this work and is a subject of future research.

In Fig. 7, the EC (bit/s/Hz) is plotted versus the PU access probability, i.e., μ. It is obvious that the EC of both systems decreases as the PU becomes more active. Moreover, it is evident that the amount of improvement due to exploiting the PU feedback increases as μ increases. As μ increases, the PU is occupying the medium more frequently and, hence, sends more packets and receives more feedback messages, and the SU senses the channel busy in more slots. Therefore, the role of feedback prevails more, and the EC gains increase. It is worth noting that even at PU activity probability of $\mu = 1$, the EC does not completely vanish. This is due to the characteristics of the interference model adopted in this section, which allows the PU and the SU to coexist, as long as the interference is within tolerable levels.

In Fig. 8, we plot the average transmit power, for both systems, versus the PU prior activity probability μ. The average transmission power decreases as the PU activity (μ) increases, since the channel becomes busy with higher probability. The SU saves power in case of the feedback-aided scheme by avoiding outage and interference with the PU if a NACK is received, as derived in (18) and (21). Assuming $P_1 = 0.5 \times W$ and $P_2 = 2 \times W$ unit power, it is shown in Fig. 8 that the SU has slightly lower average transmission power when it exploits the PU feedback.

In Fig. 9, we plotted the EC of the SU versus the transmitting power level P_1 increasing from zero to P_2. It is clear that increasing the transmitting power increases the signal-to-noise ratio for the SU TX, hence getting higher EC. On the other hand, transmitting with high power while the PU is accessing the medium will result in high interference to the PU and, hence, more NACKs due to unsuccessful packet transmissions. In turn, the SU will access the medium more with lower rates and power levels, which reduces its EC. At the extreme scenario when the SU is using $P_1 = P_2$, the no-feedback and feedback systems return the same EC as the SU is not properly responding to the PU NACKs overheard and totally ignoring it.

Next, we characterize the EC for both access schemes under the simpler collision model widely adopted in the literature and show its limitations.

V. Effective Capacity Analysis Under the Collision Model

Here, we shift our attention to the collision model, which is widely adopted in the literature due to its simplicity. However, in our problem context, we unveil a fundamental shortcoming of the this model, which completely precludes any EC benefits attributed to exploiting the PU feedback. Under the collision model, the SU senses the channel at the beginning of each time slot. If the channel is sensed idle, the SU transmits packets with fixed power level P and rate r. On the other hand, if the channel is sensed busy, the SU backs off in this time slot, and hence, it is a pure interweave CR scheme. Along the lines of Section IV, we compare two SU access schemes, namely, a system with no-feedback exploitation and a feedback-aided scheme. The EC is characterized for both systems based on (9).

A. No-Feedback Exploitation (Baseline)

In this case, we propose a six-state Markov chain where the first four states capture all possible sensing outcomes (B-B, MD, FA, and I-I).

The PU is assumed to be active with probability μ. States 5 and 6 model the (B-B) and (MD) cases, respectively, when the PU retransmits data after suffering an outage event [i.e., the PU occupies the channel with probability Pr(outage)]. Therefore, the system occupies one of the last two states in the next time slot, if and only if the PU channel is in outage in the current time slot.

Let $p_{i,j}$ denote the transition probability from state i to state j. The Markov chain modeling the system is shown in Fig. 10. The state transition probability matrix for the no-feedback exploitation scheme R_N is given by (22), shown at the bottom of the page, where $p_1 = \mu P_d$, $p_2 = \mu(1-P_d)$, $p_3 = (1-\mu)P_f$, $p_4 = (1-\mu)(1-P_f)$, and $\overline{\Pr(\text{NACK})} = 1 - \Pr(\text{NACK})$. Now, we have completely specified the transition probability matrix, i.e., $\mathbf{R}_N$, for $M = 6$ states.

To fully characterize the EC of the no-feedback exploitation scheme under the collision model, we need to get the maximum eigenvalue of the matrix $\mathbf{D}(-\theta)\mathbf{R_N}$, which can be expressed as

$$\text{EC}(\theta) = -\frac{\Lambda(\theta)}{-\theta} = \frac{-1}{\theta}\log_e sp\left(\mathbf{D}(-\theta)\mathbf{R_N}\right) \qquad (23)$$

where $\mathbf{D}(-\theta) = \mathbf{diag}\{1, 1, 1, e^{-(T-\tau)\theta r}, 1, 1\}$, r denotes the rate used by the SU, and θ is the delay exponent as pointed out in Section II.

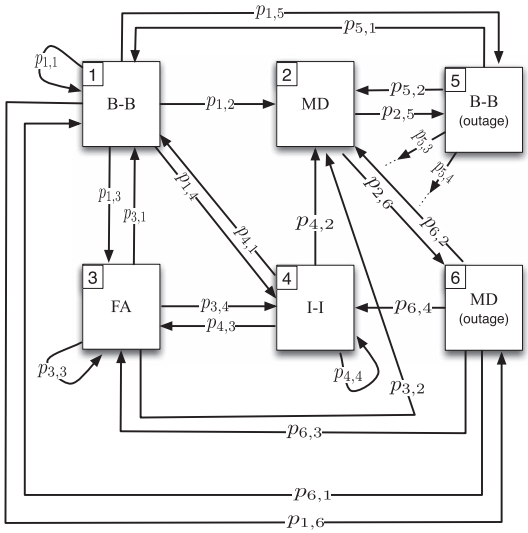

Fig. 10. Markov chain of the no-feedback exploitation system under the collision model.

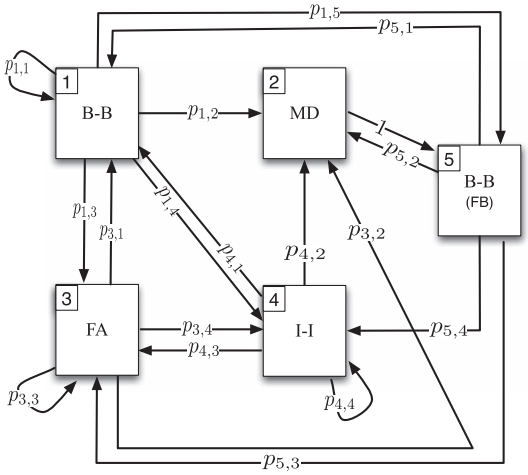

Fig. 11. Markov chain of the feedback-aided system under the collision model.

B. Feedback-Aided Scheme

Here, we analyze the EC under the collision model when the SU exploits the PU feedback messages. It is shown that the dynamics of this system are modeled as a five-state Markov chain shown in Fig. 11, as opposed to the six-state Markov chain of the no-feedback exploitation scheme. Once more, the first four states capture all possible channel sensing outcomes (B-B, MD, FA, and I-I), and the last state represents the case of "no sensing," whereby the SU overhears a "NACK" message

$$\mathbf{R}_N = \begin{bmatrix} p_1\overline{\Pr(\text{NACK})} & p_2\overline{\Pr(\text{NACK})} & p_3\overline{\Pr(\text{NACK})} & p_4\overline{\Pr(\text{NACK})} & p_d\Pr(\text{NACK}) & (1-p_d)(\Pr(\text{NACK})) \\ 0 & 0 & 0 & 0 & p_d & 1-p_d \\ p_1 & p_2 & p_3 & p_4 & 0 & 0 \\ p_1 & p_2 & p_3 & p_4 & 0 & 0 \\ p_1 & p_2 & p_3 & p_4 & 0 & 0 \\ p_1 & p_2 & p_3 & p_4 & 0 & 0 \end{bmatrix} \qquad (22)$$

from the PU receiver. The SU successfully transmits with rate r only at state 4 (I-I), at which the channel is idle and sensed idle, and backs off or causes a collision otherwise. The state transition probability matrix of the feedback-aided scheme, i.e., R_F, is given by (24), shown at the bottom of the page.

Again, to characterize the EC of the feedback-aided CR link under the collision model, we need to find the maximum eigenvalue for matrix $\mathbf{D}(-\theta)\mathbf{R}$, where $\mathbf{D}(-\theta) = \mathbf{diag}\{1, 1, 1, e^{-(T-\tau)\theta r}, 1\}$. Finally, the following theorem establishes a fundamental result that constitutes a major contribution of this paper.

Theorem 2: Under the collision model, the EC of the feedback-aided system is equal to the EC of the no-feedback exploitation system.

This result is proven in Appendix B.

C. Average Transmission Power

In terms of power, the SU will save transmission power in the feedback-aided system by avoiding sure collisions with the PU transmissions, due to overhearing NACK messages. This can be shown as follows. The average SU transmission power for the feedback-aided scheme is given by

$$P_{avg_F} = P.\{\pi_2 + \pi_4\}. \tag{25}$$

On the other hand, the average transmission power for the system with no-feedback exploitation is given by

$$P_{avg_N} = P.\{\pi_2 + \pi_4 + \pi_6\} \tag{26}$$

where π_i is the steady-state probability of state i, and P is the SU transmission power.

D. Numerical Results

Fig. 12 shows the EC of the secondary link, under the no-feedback exploitation and feedback-aided access schemes, versus the delay exponent, i.e., θ, under the collision model. These results are generated using the following system parameters: $T = 0.1$ ms, $\tau = 0.3 \times T$ s, $W = 20$ MHz, $r = 27$ Mb/s, $\mu = 0.7$, $\lambda = 1.85$, $\sigma^2_{I_p} = 1$, $\sigma^2_n = 1$, and $P_1/W = 0.05$ w/Hz. It is evident that the EC decays as delay exponent θ increases. This result agrees with intuition since more stringent delay requirements give rise to a reduced EC. Second, it is evident in Fig. 12 that there is no EC gain attributed to the feedback exploitation in the collision model. This can be easily justified by the fact that in the case of overhearing a NACK from the PU receiver, the SU backs off in the next slot and, hence, has no gain from that slot in terms of rate. Considering the system with no feedback, the SU does not receive any gain from this slot if it collides with the PU or if it correctly senses the channel to be busy. Thus, the PU feedback provides no gain to the SUs in terms of rates, under the collision model. In Appendix B, we prove this result for Theorem 2.

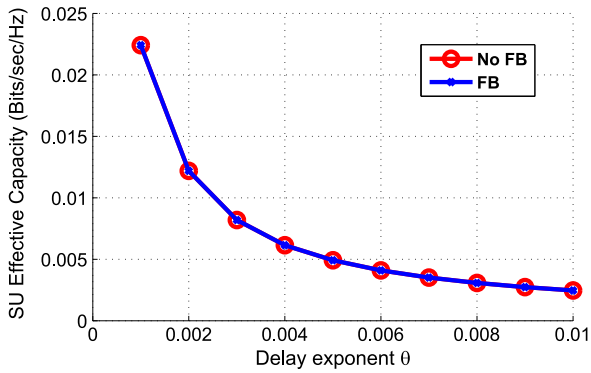

Fig. 12. EC for the feedback-aided and no-feedback exploitation schemes under the collision model.

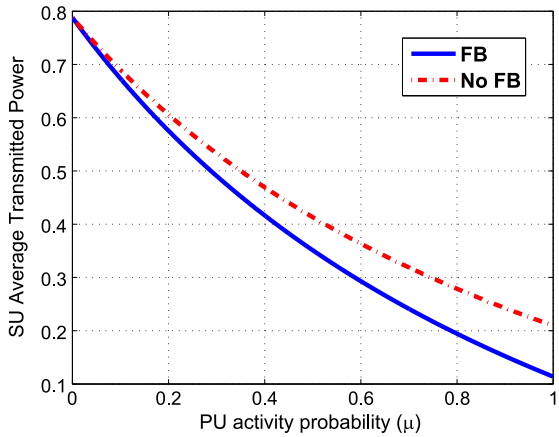

Fig. 13. Average SU transmission power for the feedback-aided and no-feedback exploitation schemes under the collision model.

Fig. 13 plots the average SU transmission power versus the PU activity μ, for the no-feedback exploitation and feedback-aided access schemes, under the collision model. Few comments are in order. First, the average SU transmission power is independent of the QoS exponent, i.e., θ; however, it decays with μ as the PU uses the medium more frequently. This is attributed to the fixed power policy used by the SU transmitter. Second, the power saving under the feedback-aided scheme is directly attributed to avoiding sure collisions upon overhearing a NACK. This is in contrast to the system that does not exploit the PU feedback where incorrect sensing results in wasted

$$\mathbf{R}_F = \begin{bmatrix} p_1\left(\overline{\Pr(\text{NACK})}\right) & p_2\left(\overline{\Pr(\text{NACK})}\right) & p_3\left(\overline{\Pr(\text{NACK})}\right) & p_4\left(\overline{\Pr(\text{NACK})}\right) & \Pr(\text{NACK}) \\ 0 & 0 & 0 & 0 & 1 \\ p_1 & p_2 & p_3 & p_4 & 0 \\ p_1 & p_2 & p_3 & p_4 & 0 \\ p_1 & p_2 & p_3 & p_4 & 0 \end{bmatrix} \tag{24}$$

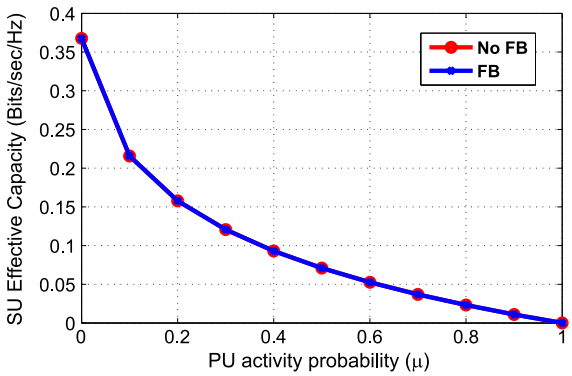

Fig. 14. EC versus PU activity probability μ under the collision model.

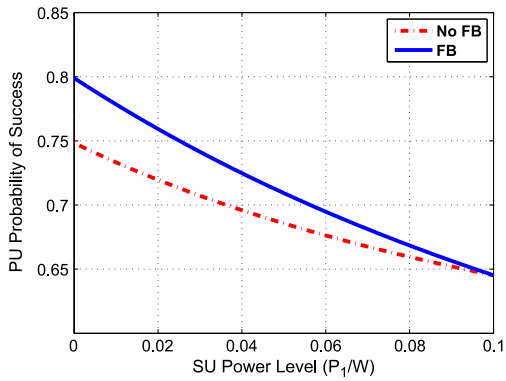

Fig. 15. PU success probability versus SU power level P_1 (P_1 from 0 to P_2).

power, particularly in the misdetection cases (i.e., states 2 and 6). In the feedback-aided system, the power is wasted only in state 2.

Fig. 14 shows the relation between the SU EC and the PU activity probability (μ). It can be explained in a manner similar to the interference model in Section IV-C; however, the PU feedback exploitation does not contribute EC gains under the collision model, as previously discussed.

In the following section, we analyze the proposed feedback-aided access scheme from the PU perspective.

VI. Primary User Performance Analysis

Analyzing the PU performance is of paramount importance to ensure that the proposed SU access scheme does not adversely affect the PU. Toward this objective, we characterize the PU success rate under the SINR interference model, in the cases of PU feedback-aided and no-feedback exploitation schemes. Since the PU feedback exploitation is considered a sensing error rectifier, we expect that if the SU overhears and utilizes the PU feedback messages, the PU will suffer less interference or, at most, the same interference level, whereas the SU gains in terms of both the EC and power saving, as previously demonstrated.

Assuming that the primary channel and the channel between the SU transmitter and the PU receiver are independent Rayleigh fading channels, we can show that the probability that the PU receiver successfully decodes its packets, conditioned on the SU power, is given by

$$\Pr(\text{Success}|P_{\text{sec}}) = e^{-\delta_{pp} r_p N_0/P_p}\left(\frac{1}{1+\frac{\delta_{pp}P_{\text{sec}}r_p}{P_p\delta_{sp}}}\right) \quad (27)$$

where P_p and P_{sec} are the PU and SU power levels, respectively, and r_P is the PU transmission rate. Note that P_{sec} takes two values, i.e., P_1 and P_2, depending on the SU sensing decision. The channel power gains for the primary link and between the SU transmitter and the PU receiver are exponentially distributed with parameters δ_{pp} and δ_{sp}, respectively. We set $\delta_{pp} = \delta_{sp} = 0.1$ for the numerical results depicted later.

Given the conditional PU success probability (conditioned on the SU power), we can directly characterize the PU success probability as follows:

$$\Pr(\text{Success}) = \sum_{P_{\text{sec}}} \Pr(\text{Success}|P_{\text{sec}}) \times \Pr(P_{\text{sec}}),\ P_{\text{sec}} = P_1, P_2. \quad (28)$$

$\Pr(P_{\text{sec}})$ depends on the SU system dynamics and the steady-state distribution of the Markov chain. In particular, the SU transmits with power level P_1 when the PU is sensed to be active and with power level P_2 when it is sensed idle, as discussed in Section IV, under the no-feedback exploitation scheme. For the feedback-aided scheme, the SU transmits with power P_1 if the PU is sensed to be active or if the SU overhears a NACK message and transmits with power P_2 when the PU is sensed idle. Next, we show how $\Pr(P_{\text{sec}})$ can be computed for the no-feedback exploitation scheme. Computing $\Pr(P_{\text{sec}})$ for the feedback-aided scheme would follow the same steps and is omitted due to space limitations. Thus

$$\Pr(P_{\text{sec}} = P_1) = \frac{\sum_{i=1,2,9,10}\pi_i}{\beta} \quad (29)$$

$$\Pr(P_{\text{sec}} = P_2) = \frac{\sum_{i=3,4,11,12}\pi_i}{\beta} \quad (30)$$

where π_i is the steady-state distribution of the system Markov chain shown in Fig. 2. Note that the PU success probability is meaningful only in the states where the PU is active. Therefore, in the last two expressions, we sum up over the states where the PU is active and divide by the normalization factor $\beta = \sum_{i=1,\ldots,4,9,\ldots,12}\pi_i$, which is the sum of state probabilities over those states.

So far, we have characterized the PU success probability. Next, we present numerical results to better understand the interaction between the SU and PU performance.

In addition, we plotted the PU success probability P_1 in Fig. 15. As P_1 increases from zero to P_2, we notice that the PU success probability decreases, since raising P_1 causes more interference to the PU. However, exploiting the PU feedback messages by the SU does not degrade the PU probability of success. More interestingly, the feedback-aided scheme used by the SU results in less interference to the PU and, hence, higher PU success probability. Therefore, we conclude that the SU power level selection, i.e., P_1 and P_2, has a direct impact on the PU performance.

VII. Conclusion and Future Work

In this paper, we have analyzed the EC of a CRN under statistical QoS constraints. We prove analytically that exploiting the primary-receiver feedback overheard at the secondary transmitter yields performance gains, in terms of the SU EC and power savings, under the interference model. However, under the simpler collision model for the same system, the PU feedback exploitation does not enhance the SU EC. In addition, we showed that the PU feedback exploitation slightly reduces the SU average transmission power under both interference models. This work can be extended along multiple directions. First, modeling and characterizing the EC for a system of multiple SUs. Second, assessing and quantifying the potential EC gains of cognitive relays along with PU feedback exploitation. In addition, quantifying the effect of error-prone feedback messages on the EC is another potential thrust for extending this work.

Appendix A

First, we quantify the EC for the no-feedback exploitation (baseline) system and then extend the analysis to the feedback-aided system, for comparison. The EC of the system is governed by the spectral radius of matrix $\mathbf{D}_N(-\theta)\mathbf{R}_N$.[3] From linear algebra, the spectral radius of a matrix is the maximum absolute eigenvalue. The matrix $\mathbf{D}_N(-\theta)\mathbf{R}_N$ is given by

$$\mathbf{D}_N(-\theta)\mathbf{R}_N = \begin{bmatrix} a_1k_1\mathbf{v} & k_1p_{1,9} & k_1p_{1,10} & k_1p_{1,11} & k_1p_{1,12} \\ a_1\mathbf{v} & p_{2,9} & p_{2,10} & p_{2,11} & p_{2,12} \\ a_2k_2\mathbf{v} & k_2p_{3,9} & k_2p_{3,10} & k_2p_{3,11} & k_2p_{3,12} \\ a_2\mathbf{v} & p_{4,9} & p_{4,10} & p_{4,11} & p_{4,12} \\ k_1\mathbf{v} & 0 & 0 & 0 & 0 \\ \mathbf{v} & 0 & 0 & 0 & 0 \\ k_2\mathbf{v} & 0 & 0 & 0 & 0 \\ \mathbf{v} & 0 & 0 & 0 & 0 \\ k_1\mathbf{v} & 0 & 0 & 0 & 0 \\ \mathbf{v} & 0 & 0 & 0 & 0 \\ k_2\mathbf{v} & 0 & 0 & 0 & 0 \\ \mathbf{v} & 0 & 0 & 0 & 0 \end{bmatrix} \tag{31}$$

where $\mathbf{v}=[p_1\ p_2\ p_3\ p_4\ p_5\ p_6\ p_7\ p_8]$, $a_1=1-\Pr(\text{NACK}')$, $a_2=1-\Pr(\text{NACK}'')$, $k_1=e^{(-(T-\tau)r_1\theta)}$, and $k_2=e^{(-(T-\tau)r_2\theta)}$. From linear algebra, the eigenvalue basic equation is given by

$$\mathbf{w}\mathbf{D}_N(-\theta)\mathbf{R}_N = \lambda_N\mathbf{w} \tag{32}$$

[3]The subscript τ refers to no feedback.

where $\mathbf{w}=[w_1\ w_2\ w_3\ \cdots\ w_{12}]$ is the eigenvector corresponding to the eigenvalue λ_N of matrix $\mathbf{D}_N(-\theta)\mathbf{R}_N$. Performing matrix multiplication in (32), we obtain

$$\begin{aligned}\lambda_N w_1 = {} & a_1k_1w_1p_1 + a_1w_2p_1 + a_2k_2w_3p_1 + a_2w_4p_1 \\ & + k_1w_5p_1 + w_6p_1 + k_2w_7p_1 + w_8p_1 + k_1w_9p_1 \\ & + w_{10}p_1 + k_2w_{11}p_1 + w_{12}p_1\end{aligned} \tag{33}$$

or, equivalently, $c_1p_1 = \lambda_N w_1$, where

$$\begin{aligned}c_1 = {} & a_1k_1w_1 + a_1w_2 + a_2k_2w_3 + a_2w_4 + k_1w_5 + w_6 \\ & + k_2w_7 + w_8 + k_1w_9 + w_{10} + k_2w_{11} + w_{12}.\end{aligned} \tag{34}$$

Similarly, it can be shown that $c_1p_2 = \lambda_N w_2$.

In general, $c_1p_m = \lambda_N w_m \quad m = 1, 2, \ldots, 8$. Moreover, we have

$$k_1p_{1,9}w_1 + p_{2,9}w_2 + k_2p_{3,9}w_3 + p_{4,9}w_4 = \lambda_N w_9 \tag{35}$$

from which we can get

$$w_9 = \frac{k_1p_{1,9}w_1 + p_{2,9}w_2 + k_2p_{3,9}w_3 + p_{4,9}w_4}{\lambda_N}. \tag{36}$$

Similarly

$$w_{10} = \frac{k_1p_{1,10}w_1 + p_{2,10}w_2 + k_2p_{3,10}w_3 + p_{4,10}w_4}{\lambda_N} \tag{37}$$

$$w_{11} = \frac{k_1p_{1,11}w_1 + p_{2,11}w_2 + k_2p_{3,11}w_3 + p_{4,11}w_4}{\lambda_N} \tag{38}$$

$$w_{12} = \frac{k_1p_{1,12}w_1 + p_{2,12}w_2 + k_2p_{3,12}w_3 + p_{4,12}w_4}{\lambda_N}. \tag{39}$$

Substituting for w_9, w_{10}, w_{11}, and w_{12} into the expression of c_1 in (34), we get (40), shown at the bottom of the page. Using the expression for c_1 from (40), we can express $c_1\lambda_N$ as given in (41), shown at the bottom of the next page. Substituting by $\lambda_N w_m = c_1p_m$, $m = 1, 2, \ldots, 8$, in (41) results in (42), shown at the bottom of the next page. For nonnegative matrices, the spectral radius, as well as the eigenvector corresponding to it, are positive according to the Perron–Frobenius theorem [26]. This implies that $c_1 \neq 0$ for the spectral radius, and hence, it can

$$\begin{aligned}c_1 = {} & \left(a_1k_1 + \frac{k_1^2p_{1,9} + k_1p_{1,10} + k_1k_2p_{1,11} + k_1p_{1,12}}{\lambda_N}\right)w_1 + \left(a_1 + \frac{k_1p_{2,9} + p_{2,10} + k_2p_{2,11} + p_{2,12}}{\lambda_N}\right)w_2 \\ & + \left(a_2k_2 + \frac{k_1k_2p_{3,9} + k_2p_{3,10} + k_2^2p_{3,11} + k_2p_{3,12}}{\lambda_N}\right)w_3 + \left(a_2 + \frac{k_1p_{4,9} + p_{4,10} + k_2p_{4,11} + p_{4,12}}{\lambda_N}\right)w_4 \\ & + k_1w_5 + w_6 + k_2w_7 + w_8\end{aligned} \tag{40}$$

be canceled from both sides of the last equation. Constructing a second-order equation in λ_N as follows:

$$\lambda_N^2 - a'\lambda_N - b' = 0. \tag{43}$$

It is clear that a' and b' are in terms of a_1, a_2, k_1, k_2, and $p_1, \ldots, p_8$; however, for now, we focus only on b', i.e.,

$$\begin{aligned} b' = &\left(k_1^2 p_{1,9} + k_1 p_{1,10} + k_1 k_2 p_{1,11} + k_1 p_{1,12}\right) p_1 \\ &+ (k_1 p_{2,9} + p_{2,10} + k_2 p_{2,11} + p_{2,12}) p_2 \\ &+ \left(k_1 k_2 p_{3,9} + k_2 p_{3,10} + k_2^2 p_{3,11} + k_2 p_{3,12}\right) p_3 \\ &+ (k_1 p_{4,9} + p_{4,10} + k_2 p_{4,11} + p_{4,12})\, p_4. \end{aligned} \tag{44}$$

To complete the proof, we now shift our attention to the feedback-aided system. Characterizing the EC through the eigenvalue of matrix $\mathbf{D}_F(-\theta)\mathbf{R}_F$.[4] Along the same lines of the no-feedback case, we have

$$\hat{\mathbf{w}}\mathbf{D}_F(-\theta)\mathbf{R}_F = \lambda_F \hat{\mathbf{w}}, \quad \hat{\mathbf{w}} = [\hat{w}_1 \quad \hat{w}_2 \quad \hat{w}_3 \quad \cdots \quad \hat{w}_{10}] \tag{45}$$

$$\mathbf{D}_F(-\theta)\mathbf{R}_F = \begin{bmatrix} a_1 k_1 \mathbf{v} & k_1 \hat{p}_{1,9} & k_1 \hat{p}_{1,10} \\ a_1 \mathbf{v} & \hat{p}_{2,9} & \hat{p}_{2,10} \\ a_2 k_2 \mathbf{v} & k_2 \hat{p}_{3,9} & k_2 \hat{p}_{3,10} \\ a_2 \mathbf{v} & \hat{p}_{4,9} & \hat{p}_{4,10} \\ k_1 \mathbf{v} & 0 & 0 \\ \mathbf{v} & 0 & 0 \\ k_2 \mathbf{v} & 0 & 0 \\ \mathbf{v} & 0 & 0 \\ k_1 \mathbf{v} & 0 & 0 \\ \mathbf{v} & 0 & 0 \\ k_2 \mathbf{v} & 0 & 0 \\ \mathbf{v} & 0 & 0 \end{bmatrix}. \tag{46}$$

[4]The subscript F refers to feedback.

Similarly, we write the matrix multiplication output as follows:

$$\hat{c}_1 \hat{p}_m = \lambda_F \hat{w}_m \quad m = 1, 2, \ldots, 8 \tag{47}$$

$$\hat{w}_9 = \frac{k_1 \hat{p}_{1,9} \hat{w}_1 + \hat{p}_{2,9} \hat{w}_2 + k_2 \hat{p}_{3,9} \hat{w}_3 + \hat{p}_{4,9} \hat{w}_4}{\lambda_F} \tag{48}$$

$$\hat{w}_{10} = \frac{k_1 \hat{p}_{1,10} \hat{w}_1 + \hat{p}_{2,10} \hat{w}_2 + k_2 \hat{p}_{3,10} \hat{w}_3 + \hat{p}_{4,10} \hat{w}_4}{\lambda_F} \tag{49}$$

$$\begin{aligned} \hat{c}_1 = &\left(a_1 k_1 + \frac{k_1^2 \hat{p}_{1,9} + k_1 \hat{p}_{1,10}}{\lambda_F}\right) \hat{w}_1 \\ &+ \left(a_1 + \frac{k_1 \hat{p}_{2,9} + \hat{p}_{2,10} +}{\lambda_F}\right) \hat{w}_2 \\ &+ \left(a_2 k_2 + \frac{k_1 k_2 \hat{p}_{3,9} + k_2 \hat{p}_{3,10}}{\lambda_F}\right) \hat{w}_3 \\ &+ \left(a_2 + \frac{k_1 \hat{p}_{4,9} + \hat{p}_{4,10}}{\lambda_F}\right) \hat{w}_4 \\ &+ k_1 \hat{w}_5 + \hat{w}_6 + k_2 \hat{w}_7 + \hat{w}_8. \end{aligned} \tag{50}$$

Following the same steps in the no-feedback system, we construct a quadratic equation in λ_F as follows:

$$\lambda_F^2 - a''\lambda_F - b'' = 0 \tag{51}$$

$$\begin{aligned} b'' = &\left(k_1^2 \hat{p}_{1,9} + k_1 \hat{p}_{1,10}\right) p_1 + (k_1 \hat{p}_{2,9} + \hat{p}_{2,10})\, p_2 \\ &+ (k_1 k_2 \hat{p}_{3,9} + k_2 \hat{p}_{3,10}) p_3 + (k_1 \hat{p}_{4,9} + \hat{p}_{4,10})\, p_4. \end{aligned} \tag{52}$$

Writing a', a'', b' and b'' in terms of the nonnegative quantities $a_1, a_2, k_1 k_2$ and transition probabilities, we find that $a' = a'' > 0$. On the other hand, $b' > b''$, which directly implies from (43) and (51) that $\lambda_N > \lambda_F$ (i.e., the spectral radius of the feedback-aided system is lower and, hence, gives higher EC), since the EC is proportional to $-\log$(spectral radius), as given in (9).

APPENDIX B

Now, we quantify the EC for the no-feedback exploitation (baseline) system and the feedback-aided system under the

$$\begin{aligned} c_1 \lambda_N = &\left(a_1 k_1 + \frac{k_1^2 p_{1,9} + k_1 p_{1,10} + k_1 k_2 p_{1,11} + k_1 p_{1,12}}{\lambda_N}\right) \times \lambda_N w_1 + \left(a_1 + \frac{k_1 p_{2,9} + p_{2,10} + k_2 p_{2,11} + p_{2,12}}{\lambda_N}\right) \times \lambda_N w_2 \\ &+ \left(a_2 k_2 + \frac{k_1 k_2 p_{3,9} + k_2 p_{3,10} + k_2^2 p_{3,11} + k_2 p_{3,12}}{\lambda_N}\right) \times \lambda_N w_3 \\ &+ \left(a_2 + \frac{k_1 p_{4,9} + p_{4,10} + k_2 p_{4,11} + p_{4,12}}{\lambda_N}\right) \times \lambda_N w_4 + k_1 \times \lambda_N w_5 + \lambda_N w_6 + k_2 \times \lambda_N w_7 + \lambda_N w_8 \end{aligned} \tag{41}$$

$$\begin{aligned} c_1 \Bigg[&\left(a_1 k_1 + \frac{k_1^2 p_{1,9} + k_1 p_{1,10} + k_1 k_2 p_{1,11} + k_1 p_{1,12}}{\lambda_N}\right) p_1 + \left(a_1 + \frac{k_1 p_{2,9} + p_{2,10} + k_2 p_{2,11} + p_{2,12}}{\lambda_N}\right) p_2 \\ &+ \left(a_2 k_2 + \frac{k_1 k_2 p_{3,9} + k_2 p_{3,10} + k_2^2 p_{3,11} + k_2 p_{3,12}}{\lambda_N}\right) p_3 + \left(a_2 + \frac{k_1 p_{4,9} + p_{4,10} + k_2 p_{4,11} + p_{4,12}}{\lambda_N}\right) p_4 \\ &+ k_1 p_5 + p_6 + k_2 p_7 + p_8 \Bigg] = c_1 \lambda_N \end{aligned} \tag{42}$$

collision model. The EC of the system is governed by the spectral radius of matrix $\mathbf{D}_N(-\theta)\mathbf{R}_N$. Thus

$$\mathbf{D}_N(-\theta)\mathbf{R}_N = \begin{bmatrix} a\mathbf{v} & p_{1,5} & p_{1,6} \\ 0 & p_{2,5} & p_{2,6} \\ \mathbf{v} & 0 & 0 \\ k\mathbf{v} & 0 & 0 \\ \mathbf{v} & 0 & 0 \\ \mathbf{v} & 0 & 0 \end{bmatrix} \tag{53}$$

where $\mathbf{v} = [p_1 \;\; p_2 \;\; p_3 \;\; p_4]$, $a = 1 - \Pr(\text{NACK})$, and $k = e^{(-(T-\tau)r\theta)}$. From linear algebra, the eigenvalue basic equation is

$$\mathbf{w}\mathbf{D}_N(-\theta)\mathbf{R}_N = \lambda_N \mathbf{w} \tag{54}$$

where $\mathbf{w} = [w_1 \; w_2 \; w_3 \; \cdots \; w_6]$ is the eigenvector corresponding to the eigenvalue λ_N of the matrix $\mathbf{D}_N(-\theta)\mathbf{R}_N$. Performing matrix multiplication in (54), we obtain

$$aw_1p_1 + 0 + w_3p_1 + aw_4p_1 + w_5p_1 + w_6p_1 = \lambda_N w_1. \tag{55}$$

Equivalently, $c_1p_1 = \lambda_N w_1$, where

$$c_1 = aw_1 + 0 + w_3 + kw_4 + kw_5 + w_6. \tag{56}$$

Similarly, it can be shown that $c_1p_2 = \lambda_N w_2$. In general

$$c_1p_m = \lambda_N w_m \quad m = 1, 2, 3, 4 \tag{57}$$

$$p_{1,5}w_1 + p_{2,5}w_2 = \lambda_N w_5 \tag{58}$$

$$w_5 = \frac{kp_{1,5}w_1 + p_{2,5}w_2}{\lambda_N} \tag{59}$$

$$w_6 = \frac{p_{1,6}w_1 + p_{2,6}w_2}{\lambda_N}. \tag{60}$$

Substituting for w_5 and w_6 into c_1, we get

$$c_1 = \left(a + \frac{p_{1,5} + p_{1,6}}{\lambda_N}\right) w_1 + \left(\frac{p_{2,5} + p_{2,6}}{\lambda_N}\right) w_2 + w_3 + kw_4. \tag{61}$$

Using the expression for c_1 given in (61), we can write $c_1\lambda_N$ as

$$c_1\lambda_N = \left(a + \frac{p_{1,5} + p_{1,6}}{\lambda_N}\right) \times \lambda_N w_1 + \left(\frac{p_{2,5} + p_{2,6}}{\lambda_N}\right) \lambda_N w_2 + \lambda_N w_3 + k \times \lambda_N w_4. \tag{62}$$

Substituting by $\lambda_N w_m = c_1 p_m$, $m = 1, 2, 3,$ and 4, in the last expression results in

$$c_1 \left[\left(a + \frac{p_{1,5} + p_{1,6}}{\lambda_N}\right) p_1 + \left(\frac{1}{\lambda_N}\right) p_2 + p_3 + kp_4\right] = c_1\lambda_N. \tag{63}$$

For nonnegative matrices, the spectral radius as well as the eigenvector corresponding to it are positive according to the Perron–Frobenius theorem [26]. This, in turn, implies that $c_1 \neq 0$ for the spectral radius, and hence, it can be canceled from both sides of the last equation. Forming a second-order polynomial in λ_N as follows:

$$\lambda_N^2 - a'\lambda_N - b' = 0 \tag{64}$$

where $a' = ap_1 + p_3 + kp_4$, and $b' = (p_1(p_{1,5} + p_{1,6}) + p_2)$

To complete the proof, we shift our attention to the feedback-aided system. Characterizing the EC through the eigenvalue of matrix $\mathbf{D}_F(-\theta)\mathbf{R}_F$.[5] Along the same lines of the no-feedback case, we have

$$\hat{\mathbf{w}}\mathbf{D}_F(-\theta)\mathbf{R}_F = \lambda_F \hat{\mathbf{w}}, \quad \hat{\mathbf{w}} = [\hat{w}_1 \quad \hat{w}_2 \quad \hat{w}_3 \quad \cdots \quad \hat{w}_5] \tag{65}$$

$$\mathbf{D}_F(-\theta)\mathbf{R}_F = \begin{bmatrix} a\mathbf{v} & \hat{p}_{1,5} \\ 0 & 1 \\ \mathbf{v} & 0 \\ k\mathbf{v} & 0 \\ \mathbf{v} & 0 \end{bmatrix}. \tag{66}$$

Similarly, we write the matrix multiplication output as follows:

$$\hat{c}_1\hat{p}_m = \lambda_F \hat{w}_m \quad m = 1, 2, \ldots, 4, \quad \hat{w}_5 = \frac{\hat{p}_{1,5}\hat{w}_1 + \hat{w}_2}{\lambda_F} \tag{67}$$

$$\hat{c}_1 = \left(a + \frac{\hat{p}_{1,5}}{\lambda_F}\right) \hat{w}_1 + \frac{1}{\lambda_N}\hat{w}_2 + \hat{w}_3 + k\hat{w}_4. \tag{68}$$

Following the same steps in the no-feedback system, we construct a quadratic equation in λ_F as follows:

$$\lambda_F^2 - a''\lambda_F - b'' = 0 \tag{69}$$

where $a'' = ap_1 + p_3 + kp_4$, and $b'' = (p_1\hat{p}_{1,5} + p_2)$.

From a', a'', b', and b'', it is clear that $a' = a''$ and $b' = b''$, which directly implies from (64) and (51) that $\lambda_N = \lambda_F$ (i.e., the spectral radii of both models are equal and, hence, give the same EC), since the EC is proportional to $-\log(\text{spectral radius})$, as given in (9).

ACKNOWLEDGMENT

The statements made herein are solely the responsibility of the authors.

REFERENCES

[1] A. Anwar, K. Seddik, T. Elbatt, and A. Zahran, "Effective capacity of delay constrained cognitive radio links exploiting primary feedback," in *Proc. 11th WiOpt*, May 2013, pp. 412–419.

[2] P. Kolodzy and I. Avoidance, "Spectrum policy task force," Federal Commun. Commission, Washington, DC, USA, Rep. ET Docket, no. 02-135, 2002.

[3] J. Mitola and G. Q. Maguire, Jr., "Cognitive radio: Making software radios more personal," *IEEE Pers. Commun.*, vol. 6, no. 4, pp. 13–18, Aug. 1999.

[4] S. Haykin, "Cognitive radio: Brain-empowered wireless communications," *IEEE J. Sel. Areas Commun.*, vol. 23, no. 2, pp. 201–220, Feb. 2005.

[5] I. Akyildiz, W. Lee, M. Vuran, and S. Mohanty, "Next generation/dynamic spectrum access/cognitive radio wireless networks: A survey," *Comput. Netw.*, vol. 50, no. 13, pp. 2127–2159, Sep. 2006.

[6] K. Eswaran, M. Gastpar, and K. Ramchandran, "Bits through ARQs: Spectrum sharing with a primary packet system," in *Proc. IEEE ISIT*, Jun. 2007, pp. 2171–2175.

[7] S. Huang, X. Liu, and Z. Ding, "Distributed power control for cognitive user access based on primary link control feedback," in *Proc. IEEE INFOCOM*, Mar. 2010, pp. 1–9.

[5] The subscript F refers to feedback.

[8] F. Lapiccirella, Z. Ding, and X. Liu, "Improved spectrum access control of cognitive radios based on primary ARQ signals," *IET Commun.*, vol. 6, no. 8, pp. 900–908, May 2012.
[9] A. Arafa, K. Seddik, A. Sultan, T. ElBatt, and A. El-Sherif, "A feedback—Soft sensing-based access scheme for cognitive radio networks," *IEEE Trans. Wireless Commun.*, vol. 12, no. 7, pp. 3226–3237, Jul. 2013.
[10] P. Gupta and P. Kumar, "The capacity of wireless networks," *IEEE Trans. Inf. Theory*, vol. 46, no. 2, pp. 388–404, Mar. 2000.
[11] R. Tannious and A. Nosratinia, "Cognitive radio protocols based on exploiting hybrid ARQ retransmissions," *IEEE Trans. Wireless Commun.*, vol. 9, no. 9, pp. 2833–2841, Sep. 2010.
[12] D. Wu and R. Negi, "Effective capacity: A wireless link model for support of quality of service," *IEEE Trans. Wireless Commun.*, vol. 2, no. 4, pp. 630–643, Jul. 2003.
[13] S. B. Mafra, R. D. Souza, J. L. Rebelatto, E. M. Fernandez, and H. Alves, "Cooperative overlay secondary transmissions exploiting primary retransmissions," *EURASIP J. Wireless Commun. Netw.*, vol. 2013, no. 196, pp. 1–12, Jul. 2013.
[14] C.-S. Chang and J. Thomas, "Effective bandwidth in high-speed digital networks," *IEEE J. Sel. Areas Commun.*, vol. 13, no. 6, pp. 1091–1100, Aug. 1995.
[15] L. Musavian and S. Aissa, "Effective capacity of delay-constrained cognitive radio in Nakagami fading channels," *IEEE Trans. Wireless Commun.*, vol. 9, no. 3, pp. 1054–1062, Mar. 2010.
[16] H. Tran, T. Duong, and H. Zepernick, "Queuing analysis for cognitive radio networks under peak interference power constraint," in *Proc. 6th ISWPC*, Feb. 2011, pp. 1–5.
[17] H. Tran, T. Q. Duong, and H.-J. Zepernick, "Delay performance of cognitive radio networks for point-to-point and point-to-multipoint communications," *EURASIP J. Wireless Commun. Netw.*, vol. 2012, no. 9, pp. 1–15, Dec. 2012.
[18] L. Musavian and S. Aissa, "Fundamental capacity limits of cognitive radio in fading environments with imperfect channel information," *IEEE Trans. Commun.*, vol. 57, no. 11, pp. 3472–3480, Nov. 2009.
[19] S. Akin and M. Gursoy, "Effective capacity analysis of cognitive radio channels for quality of service provisioning," *IEEE Trans. Wireless Commun.*, vol. 9, no. 11, pp. 3354–3364, Nov. 2010.
[20] D. Li, "Effective capacity limits of cognitive radio networks under peak interference constraint," in *Proc. 12th IEEE ICCT*, Nov. 2010, pp. 218–222.
[21] S. Shakkottai, "Effective capacity and QoS for wireless scheduling," *IEEE Trans. Autom. Control*, vol. 53, no. 3, pp. 749–761, Apr. 2008.
[22] T. Cover and J. Thomas, *Elements of Information Theory*. New York, NY, USA: Wiley, 2006.
[23] H. V. Poor, *An Introduction to Signal Detection and Estimation*. Berlin, Germany: Springer-Verlag, 1994.
[24] A. Goldsmith, S. Jafar, I. Maric, and S. Srinivasa, "Breaking spectrum gridlock with cognitive radios: An information theoretic perspective," *Proc. IEEE*, vol. 97, no. 5, pp. 894–914, May 2009.
[25] C. Chang, *Performance Guarantees in Communication Networks*. New York, NY, USA: Springer-Verlag, 1995.
[26] G. Frobenius, *Über Matrizen aus Nicht Negativen Elementen*. Berlin, Germany: Reimer, 1912.

Ahmed H. Anwar (S'09) received the B.Sc. degree (with highest honors) in electrical engineering from Alexandria University, Alexandria, Egypt, in 2011 and the M.Sc. degree in wireless communications from Nile University, Giza, Egypt, in 2013. He is currently working toward the Ph.D. degree with the Department of Electrical and Computer Engineering, University of Central Florida, Orlando, FL, USA. His thesis work was on quality-of-service provisioning for real-time applications in cognitive radio networks.

Between August 2013 and December 2013, he was a Research Assistant with Qatar University, Doha, Qatar. He is a member of the Digital Signal Processing Laboratory.

Karim G. Seddik (S'04–M'08–SM'14) received the B.S. (with highest honors) and M.S. degrees in electrical engineering from Alexandria University, Alexandria, Egypt, in 2001 and 2004, respectively, and the Ph.D. degree from the Department of Electrical and Computer Engineering, University of Maryland, College Park, MD, USA, in 2008.

He is an Associate Professor with the Department of Electronics and Communications Engineering, American University in Cairo (AUC), New Cairo, Egypt. Before joining AUC, he was an Assistant Professor with the Department of Electrical Engineering, Alexandria University, Alexandria, Egypt. His research interests include cooperative communications and networking, multiple-input–multiple-output orthogonal frequency-division multiplexing systems, cognitive radio, layered channel coding, and distributed detection in wireless sensor networks.

Dr. Seddik has served on the Technical Program Committee of numerous IEEE conferences in the areas of wireless networks and mobile computing. He received the Certificate of Honor from the Egyptian President for being ranked first among all the departments in College of Engineering, Alexandria University, in 2002; the Graduate School Fellowship from the University of Maryland in 2004 and 2005; and the Future Faculty Program Fellowship from the University of Maryland in 2007.

Tamer ElBatt (SM'06) received the B.S. and M.S. degrees in electronics and eommunications engineering from Cairo University, Egypt, in 1993 and 1996, respectively, and the Ph.D. degree in electrical and computer engineering from the University of Maryland, College Park, MD, USA in 2000.

From 2000 to 2009, he was with major U.S. industry R&D labs, e.g., HRL Laboratories, LLC, Malibu, CA, USA; and Lockheed Martin ATC, Palo Alto, CA, at various positions. In July 2009, he joined the Electronics and Communications Department, Faculty of Engineering, Cairo University, as an Assistant Professor, where he is currently an Associate Professor. Since 2009, he has also had a joint appointment with Nile University, Egypt, and has currently served as the Director of the Wireless Intelligent Networks Center (WINC) since October 2012. His research has been supported by the U.S. DARPA, ITIDA, FP7, General Motors, Microsoft, and Google and is currently being supported by NTRA, QNRF, H2020, and Vodafone Egypt Foundation. He has published more than 80 papers in prestigious journals and international conferences and he holds seven issued U.S. patents. His research interests lie in the broad areas of performance analysis and the design and optimization of wireless and mobile networks.

Dr. ElBatt has served on the technical program committees of numerous IEEE and ACM conferences. He served as the Demos Co-Chair of ACM Mobicom in 2013 and as the Publications Co-Chair of IEEE Globecom in 2012 and EAI Mobiquitous in 2014. He currently serves on the Editorial Board of IEEE TRANSACTIONS ON MOBILE COMPUTING and the Wiley International Journal of Satellite Communications and Networking. He was a Visiting Professor with the Department of Electronics, Politecnico di Torino, Italy, in August 2010; FENS, Sabanci University, Turkey, in August 2013; and the Department of Information Engineering, University of Padova, Italy, in August 2015. He received the 2014 State Incentive Award in Engineering Sciences and the 2012 Cairo University Incentive Award in Engineering Sciences.

Ahmed H. Zahran (M'11) received the B.Sc. and M.Sc. degrees in electrical engineering from the Department of Electronics and Electrical Communication, Faculty of Engineering, Cairo University, Giza, Egypt, in 2000 and 2002, respectively, and the Ph.D. degree with the Department of Electrical and Computer Engineering, University of Toronto, Toronto, ON, Canada, in 2007.

He is an Assistant Professor with the Department of Electronics and Electrical Communications, Faculty of Engineering, Cairo University. He is currently on a sabbatical leave with the MISL Group, Department of Computer Science, University College Cork, Cork, Ireland. He was previously with Nile University, Giza, as an Adjunct Assistant Professor. His research interests span different topics in wireless mobile networking, such as multimedia streaming, cognitive networking, energy-efficient networking, mobility and resource management, and modeling and performance evaluation.